Journal of Sustainability Science and Management
Volume 18 Number 8, August 2023: 125-141
eISSN: 2672-7226

TRAPPED SEDIMENT IN SEAGRASS ECOSYSTEM: BINTAN ISLAND

DEWI SURINATI*, ULUNG JANTAMA WISHA, AHMAD BAYHAQI, HANIF BUDI PRAYITNO AND SUSI RAHMAWATI

Research Center for Oceanography, National Research and Innovation Agency, 10340 Jakarta, Indonesia.

**Corresponding author: dewi.surinati@gmail.com*
Submitted final draft: 2 March 2023 *Accepted: 16 April 2023* http://doi.org/10.46754/jssm.2023.08.009

Abstract: This study attempts to figure out the physical characteristics of water in the surrounding Bintan Island and considers the role of the seagrass ecosystem in trapping sediment transport using model simulation. Field observation was conducted during the first transitional monsoon to collect the ocean current data and Total Suspended Solids (TSS) at the three observation stations (Pengudang, Teluk Bakau, and Madong). A hydrodynamic flow model was employed to simulate the current pattern and sediment transport. Based on the simulation result, the existence of seagrass meadows in the Pengudang and Madong areas could significantly trap the sediment and induce sedimentation. Of particular concern, it is predicted that sediment transport in all stations will gradually decrease by about 15% per year throughout 2019-2023. This prediction was applied without any further changes in water conditions in Bintan Island so that different results could be potentially gained according to many factors influencing the movement of sediment.

Keywords: Seagrass, trapped sediment, Bintan Island.

Introduction

As a critical coastal zone ecosystem, seagrass is essential for coastal communities. Ecologically, seagrass provides the organic and inorganic compounds for biota and is home to many valuable fishes, playing a significant role as feeding and nursery ground for them. The presence of seagrass meadows in the coastal area is essential, shaping the coastal zone as the most productive system in the globe and being a barrier from robust waves and currents (coastal protection) (Supriyadi *et al.,* 2018). Of particular concern, seagrass meadows can potentially induce sediment trapping (Moriarty & Boon, 1989), preventing coastal erosion or sedimentation.

On the other hand, the seagrass meadow is very sensitive toward the climate change issue (Harley *et al.*, 2006) and massive development (Duarte, 2002; Bozec *et al*., 2008). A previous study reported that anthropogenic activities contribute to the decrease in seagrass ecosystem (Waycott *et al*., 2005; Orth *et al.*, 2006) by 7% annually, and about 30% of seagrass stock worldwide has been damaged (Brodie & N'Yeurt, 2018). In Indonesia, the seagrass meadow is nationally under pressure with the dominant threat; human activity (Wahyudin *et al.,* 2018). For example, as the largest island in the Riau Archipelago of Indonesia, the loss of seagrass meadows in Bintan Island has been reported, with the status of 11 species being damaged (Karlina *et al.,* 2018). Consequently, this condition impacts coastal instability. Therefore, a study estimating the changes in coastal systems due to seagrass area reduction is worthy of studying.

Bintan Island is the largest among the 3,200 islands of the Riau Archipelago, positioned at about 10 km in the eastern Batam Island. It is surrounded by a 105 km coastline and arranged of rolling topography in its landform. Geologically, the coastal area of Bintan Island is composed of silt-coarse sediments (Suhana *et al.,* 2018; Sarmanda *et al.,* 2018). The sediment transport along the coast relies on the coastal-current regimes, with a robust current magnitude

for certain times. The tidal type is a semidiurnal tide, and the tidal currents significantly control the coastal transport on this island (Sarmanda *et al.,* 2018). Bintan Island is geographically bordered by the South China Sea, whereby extreme weather and climate variability periodically impact this island, inducing a high intensity of land weathering (Witasari *et al.,* 2020). Because of the tremendous influence of the Climatic-Oceanographic factors on the coastal system of Bintan Island, a prediction of future possible changes in coastal instability (erosion-sedimentation) should be carried out.

As a coastal management effort, many experts study the seagrass-sediment interaction, such as their feedback interaction (De Boer, 2007), the influence of sediment on the seagrass ecosystem (Maeztu *et al.,* 2020), and the sediment rate in the seagrass meadow (Nursanti *et al.,* 2013). Several previous related studies have explicitly explained the sediment characteristics and potential pollution in Bintan Island (Hamra & Patria, 2019; Zulfikar *et al.,* 2021). However, sediment transport quantification has never been assessed to date. On the other hand, the hydro-oceanographical conditions in Bintan Island need to be more elucidated, whereas the other studies only discussed one or two specific coastal areas of Bintan Island (Suryansyah, 2013; Irawan, 2017). Moreover, based on hydrodynamic modelling, higher current magnitude was observed in the northern and eastern Bintan Island, where the flood and ebb currents predominantly control the coastal area (Bayhaqi *et al.,* 2021).

Concerning the seagrass area in Bintan Island, many studies have observed a decreasing trend over the seagrass zone (Kuriandewa & Supriyadi, 2006; Setyobudiandi & Boer, 2021). A few studies discussed the role of a seagrass meadow in trapping the sediment and its influence on sediment transport, so these aspects should be investigated. More comprehensive information is needed to figure out seagrass's role in trapping the coastal area sediment. Therefore, this study aimed to quantify the sediment transport on the Bintan Island coast using a hydrodynamic model approach to unravel the role of seagrass meadows in trapping sediment.

Materials and Methods

Data Collection

The field observation was conducted during the first transitional season monsoon 2019 (31 March to 5 April) to collect in-situ data such as the time series of ocean currents data (24 hours), which was recorded by mooring measurement using a Recording Current Meter (RCM) Aanderaa and Total Suspended Solids (TSS) to achieve the goal of this study. The ocean currents data were measured at the three stations representing each region of Bintan Island, where the TSS sampling was conducted at the same regions (Figure 1). The station names for the northern, eastern, and southwestern regions are Pengudang, Teluk Bakau, and Madong, respectively. These stations were chosen based on a consideration of the influence of the South China Sea in the east (Teluk Bakau), the Singapore Strait in the north (Pengudang), and the Malacca Strait in the southwest (Madong). 39 samples were analysed to gain TSS concentration (see Figure 1 for mooring and water sample stations). However, due to the bad weather during field observation, sampling at station 12 was cancelled, so the total number of stations was 38. The field-measured ocean current data were used to validate the hydrodynamic model simulation, and the TSS data were applied as input within the sediment transport model development (Fattah *et al*., 2018).

The explanation for the hydrodynamic and sediment transport model can be seen in the next section. Besides, bathymetry and coastline data are needed to shape a boundary in a simulation. The bathymetry and coastline were obtained from the Indonesian Navy's Hydrography and Oceanography Center (Pushidrosal) and Global Self-Continent Hierarchical High-Resolution Geography (GSHHG)-NOAA, respectively (Wessel & Smith, 1996). Furthermore, as the one of main drivers for sediment transport in the waters, the information for wave

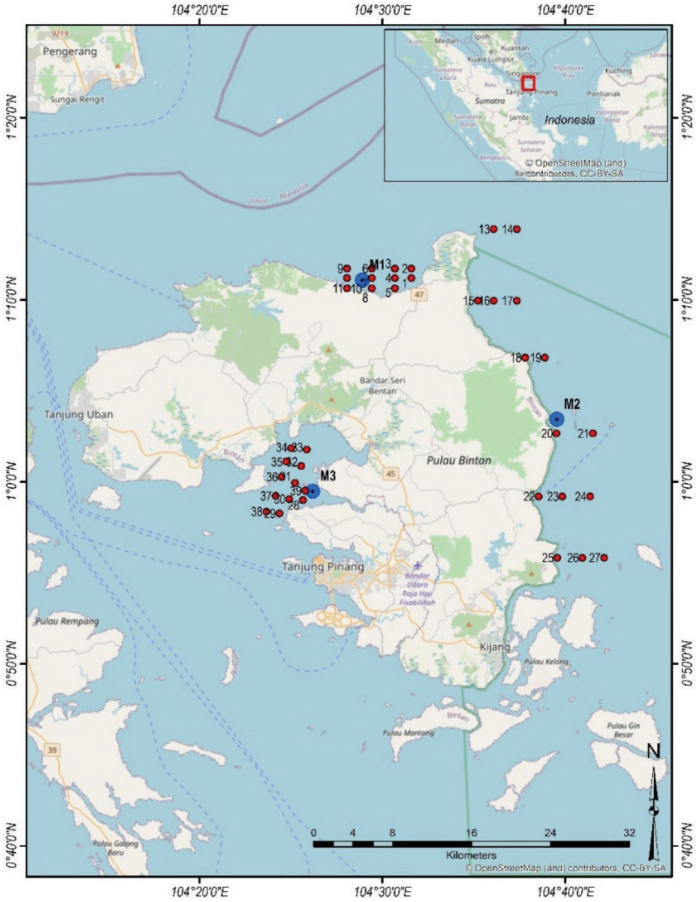

Figure 1: Map of Bintan Island with the observation points. The red circles refer to the water sampling point while the blue circles show the mooring station. Each mooring point represents the northern (M1/ Pengudang), eastern (M2/Teluk Bakau) and southwestern (M3/Madong) regions of Bintan Island

characteristics was also included in the input of model simulation. In this study, we considered the wind-generated wave data as one of the modelling inputs which was calculated from the time series data of wind from the European Center for Medium-Range Weather Forecasts (ECMWF) (Signell *et al*., 2005; Moeini *et al*., 2010). A monthly 10 m ERA5 wind data (u- and v-component) from 2009 to 2018 was employed to determine the wind variation in the study area, with a horizontal resolution of 0.25°. These data can be accessed via the following webpage: https://cds.climate.copernicus.eu/.

Hydrodynamic Model Simulation

In this study, we used an integrated model flexible mesh of MIKE 21 to analyse the mutual interaction between waves and tidal currents in the estuary using an amalgamated flow and spectral wave model (Wisha *et al*., 2018). The flow model created was based on shallow water equations in which horizontal momentum and continuity were integrated over depth as follows:

$$\frac{\partial h}{\partial t} + \frac{\partial h\bar{u}}{\partial x} + \frac{\partial h\bar{v}}{\partial y} = hS \quad (1)$$

$$\frac{\partial h\bar{u}}{\partial t}+\frac{\partial h\bar{u}^2}{\partial x}+\frac{\partial h\overline{vu}}{\partial y}=f\bar{v}h-gh\frac{\partial \eta}{\partial x}-\frac{h}{\rho_o}\frac{\partial \rho_o}{\partial x}-\frac{gh^2}{2\rho_o}\frac{\partial \rho}{\partial x}+\frac{\tau_{sx}}{\rho_o}-\frac{\tau_{bx}}{\rho_o}-\frac{1}{\rho_o}\left(\frac{\partial S_{xx}}{\partial x}+\frac{\partial S_{xy}}{\partial y}\right)+$$
$$\frac{\partial}{\partial x}(hT_{xx})+\frac{\partial}{\partial y}(hT_{xy})+hu_sS \quad (2)$$

$$\frac{\partial h\bar{v}}{\partial t}+\frac{\partial h\overline{uv}}{\partial x}+\frac{\partial h\bar{v}^2}{\partial y}=f\bar{u}h-gh\frac{\partial \eta}{\partial y}-\frac{h}{\rho_o}\frac{\partial \rho_o}{\partial y}-\frac{gh^2}{2\rho_o}\frac{\partial \rho}{\partial y}+\frac{\tau_{sy}}{\rho_o}-\frac{\tau_{by}}{\rho_o}-\frac{1}{\rho_o}\left(\frac{\partial S_{yx}}{\partial x}+\frac{\partial S_{yy}}{\partial y}\right)+$$
$$\frac{\partial}{\partial x}(hT_{xy})+\frac{\partial}{\partial y}(hT_{yy})+hv_sS \quad (3)$$

where:

t = time (s),
x,y = cartesian coordinates,
η = surface elevation (m),
d = still water depth (m),
h = total water depth (m),
f = coriolis Parameter,
g = gravitational acceleration,
ρ = water density (kg/m^3),
S_{xx},S_{xy},S_{yx}, and S_{yy} = radiation stress tensor components,
ρ_O = reference density of water (kg/m^3),
S = discharge magnitude in the source point,
u_s and v_s = velocity within an ambient state of water (m/s),
$\bar{u}$ and $\bar{v}$ = depth-averaged velocities (m/s),
τ_{sx},τ_{sy},τ_{bx}, and τ_{by} = the x and y components of the surface wind and bottom shear stresses,
T_{ij} = the lateral stresses including viscous friction, turbulent friction, and differential advection, estimated using an eddy viscosity (A) formulation based on the depth average velocity gradients,

$$T_{xx}=2A\frac{\partial \bar{u}}{\partial x},T_{xy}=A\left(\frac{\partial \bar{u}}{\partial y}+\frac{\partial \bar{v}}{\partial x}\right),T_{yy}=2A\frac{\partial \bar{v}}{\partial y}$$

In addition to the bottom shear stress, it is determined by a quadratic friction law, considering the drag coefficient, the flow velocity in the surface bottom, and water density (Wisha *et al.,* 2022). In this simulation, the drag coefficient is determined by a Manning number, *M*. We applied two scenarios to estimate the seagrass ability to trap the sediment (indicated by higher bed resistance) by varying the manning number (drag coefficient) of 32 m$^{1/3}$/s for an initial condition (Scenario 1) and 40 m$^{1/3}$/s for a high bed resistance condition (due to seagrass meadow) (Scenario 2).

The spectral wave model, on the other hand, was based on a parameterization of the wave action spectrum as a dependent variable. A flexible mesh was prepared just before simulating with the lowest allowable angle of 26^o and maximum node number of 100,000.

After the hydrodynamic model was simulated and validated using field-observed data. A mud transport model was prepared to be resimulated applying the previous simulation results as the input. From this simulation, we gained sediment transport in the water column and surface bottom (Solihuddin *et al.,* 2020). Model outputs were also used to calculate sediment transport along the coast employing empirical equations generated by a correlation between sediment transport and wave energy flux component to predict the sediment budget (Wisha *et al.*, 2019) as follows:

$$Q_s=\frac{K}{(\rho_s-\rho)g(1-n)}P_1 \quad (4)$$

where:

Q_S = sediment transport along the coast (m^3/s),
K = 0.39, according to significant wave height values,
ρ_S = density of sediment (kg/m^3),
n = sediment porosity,
P_1 = wave energy flux component

TSS Quantification

Seawater samples were collected from the 38 sampling stations around Bintan Island at the surface layer. The samples were then placed in 500 ml HDPE bottles and stored in a cooler box during the trip. The sample was then filtered using a *GF/F* filter paper with a pore size of 0.45 µm which had been preheated (12 hours, 450^{o}C)

and weighed. After the filtering process, the filter paper was heated to a temperature of 40°C for 24 hours. TSS (mg/L) was calculated by using the Gravimetric method (Fischer, 2016) with the following formula:

$$TSS = \frac{(W2-W1)}{Vs} \quad (5)$$

where:

W_2 = The weight of dry filter paper after filtration (mg),
W_1 = The weight of the initial filter paper (mg),
V_s = Total volume of filtered seawater sample (L)

Results and Discussion

TSS Initial Condition

Figure 2 shows the TSS distribution obtained from in-situ measurements in Bintan coastal water. TSS concentrations in the eastern, northern, and southwestern parts of Bintan Island are comparable with respective ranges of 6.80-19.20, 6.40-18.60, and 7.40-18.40 mg/L. These results are consistent with TSS concentrations reported at Port Dickson coastal waters and offshore sites of Malacca Strait with concentrations less than 100 mg/L (Bong & Lee, 2008; Balqis *et al.,* 2016). They also correspond to TSS concentration in Setiu wetland, Malaysia ranging from 1.3 to 19.7 mg/L (southern part of South China Sea) in 2001. However, the Setiu wetland exhibited lower concentrations (0.31-4.11 mg/L) in 2008 due to slow water movement during flood tides resulting in less disturbed bottom sediments (Suratman *et al*., 2014).

Concerning the TSS in Bintan Island, it tended to be higher in offshore areas (ranging from 13.48 to 18.50 mg/L), instead of near the coast in the northern part (Pengudang). By contrast, lower TSS concentrations were observed in the eastern part of Pengudang station, ranging from 6.4 to 12.52 mg/L. Higher TSS concentrations in the offshore area were also reported in the northwestern South China Sea during typhoon events. This was attributed to strong wind-induced upwelling and upper-water mixing (Li *et al.,* 2021).

Unlike the northern observation area, in the Teluk Bakau (eastern Bintan Island), low TSS concentrations were predominant in the middle observation area, ranging from 6.8 to 11.8 mg/L. It gradually increased toward the north and the south of the modelled area, reaching 19.19 mg/L (Figure 2). These states indicate that the robust water mass movement from the South China Sea is predominant in the eastern area, whereby the transport mechanism will be considerable, resulting in significant TSS transport (Suhana *et al*., 2018). On the other hand, the embayment-like system in the northern and southern Teluk Bakau area induces an eddy circulation, evoking the TSS resuspension in the upper layer (Xiang *et al.,* 2019).

In the western area of Bintan Island (Madong), the geological formation is categorised as a semi-enclosed bay, where the current motions are supposed to be weaker than the other observation areas (Wisha *et al.,* 2018). The highest TSS concentrations were observed in the mouths of several estuaries because of river runoff transport, ranging from 13.31 to 18.39 mg/L (Figure 2). TSS concentration gradually decreased toward the middle of Madong Bay, reaching 7.4 mg/L.

Model Validation

Since the model simulation we used in this study is an approach, the validation stage is imperative to ensure the model performance replicating the field condition (Cea *et al*., 2014). We validated the TSS model result, and 39 stations were compared with in situ data (Figure 3). Overall, except for stations 7 and 20, the field and model data comparison showed a similar pattern. The TSS concentration ranged from 5 to 20 mg/L. The RMSE gained from this assessment was 7.53% [Figure 3 (A)].

A linear regression analysis was also performed to determine the deviation between field-measured and simulated TSS data. Based on the correlation coefficient, these data were 81% correlated with each other, with an R^2 of 0.66 and a standard error of 2.06 [Figure 3 (B)]. Furthermore, according to the Analysis

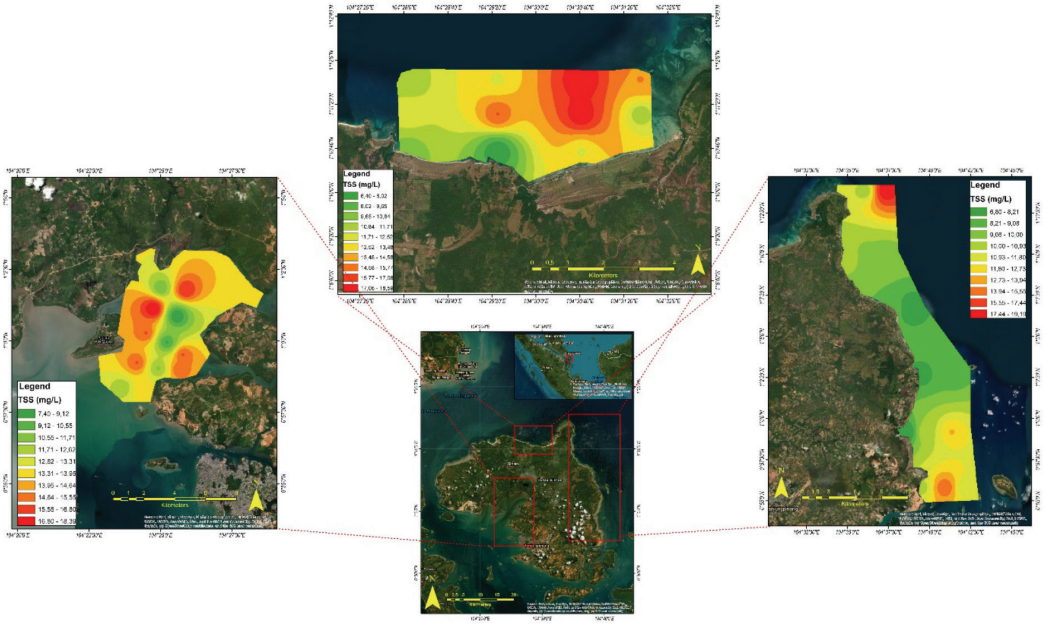

Figure 2: TSS distribution in April 2019

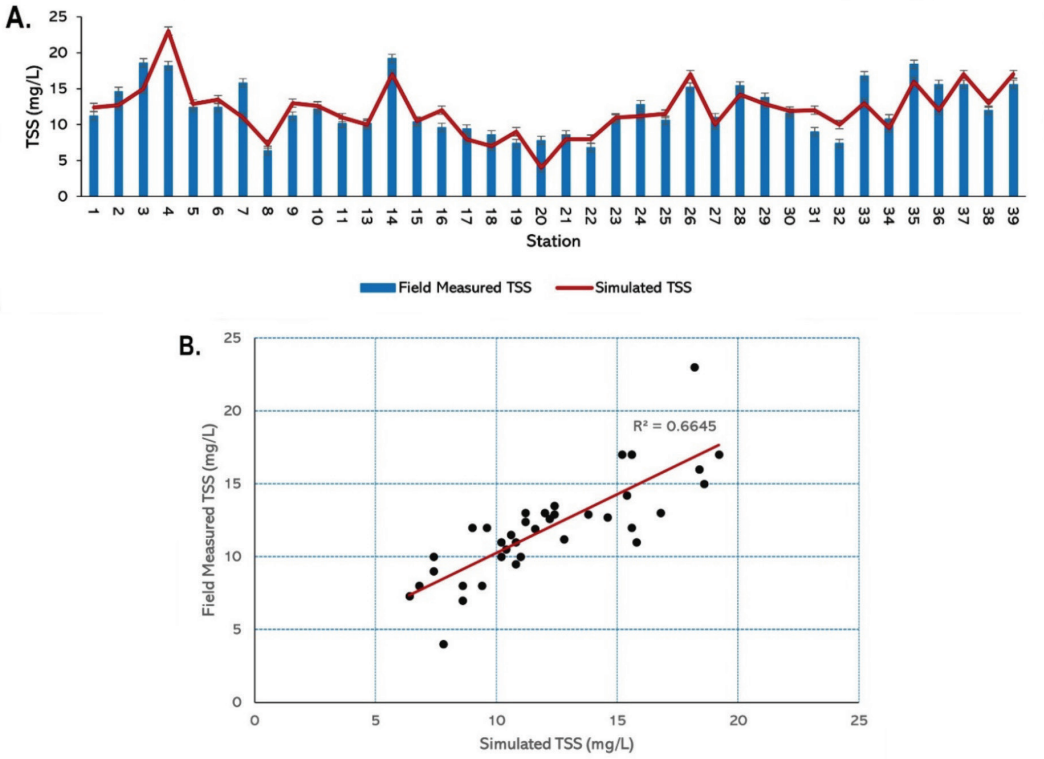

Figure 3: TSS validation between the field measurement and simulation; general TSS comparison (A); linear regression graph (B)

of Variance (ANOVA), the significance F was less than 5%, showing that the model is suitable and statistically significant. TSS simulation was performed to determine the average bed sediment turbulent and tidal current-induced scour event throughout the study area which is discussed in the following subsection.

Validation was also applied to the current velocity data. The velocity component of currents was extracted, picking up three main study areas representing the northern, eastern, and southwestern Bintan Island. In the northern part (Pengudang area), the RMSE obtained was 5.64% and 6.29% for the zonal and meridional components of current, respectively (Figure 4). The meridional component of currents shows an erratic fluctuation compared to the zonal component, illustrating that vertical transport intensively takes place in this area with a velocity ranging from -1 to 0.8 m/s. In contrast, the zonal components of current tended to be weak, with almost zero speed at certain times.

The flood tide phases coincide with the positive zonal current, indicating the easterly current predominantly moved westward during this tidal condition and vice versa during the ebb tides, where the eastward transport is more dominant. Unlike the zonal current variability, the meridional current did not follow the tidal patterns, tending to be arbitrarily erratic. The predominance of negative values of the meridional component of currents indicates that seaward transport frequently occurs where the river-sourced suspended materials will be distributed and deposited in the upper coastal zone (Wisha *et al*., 2022).

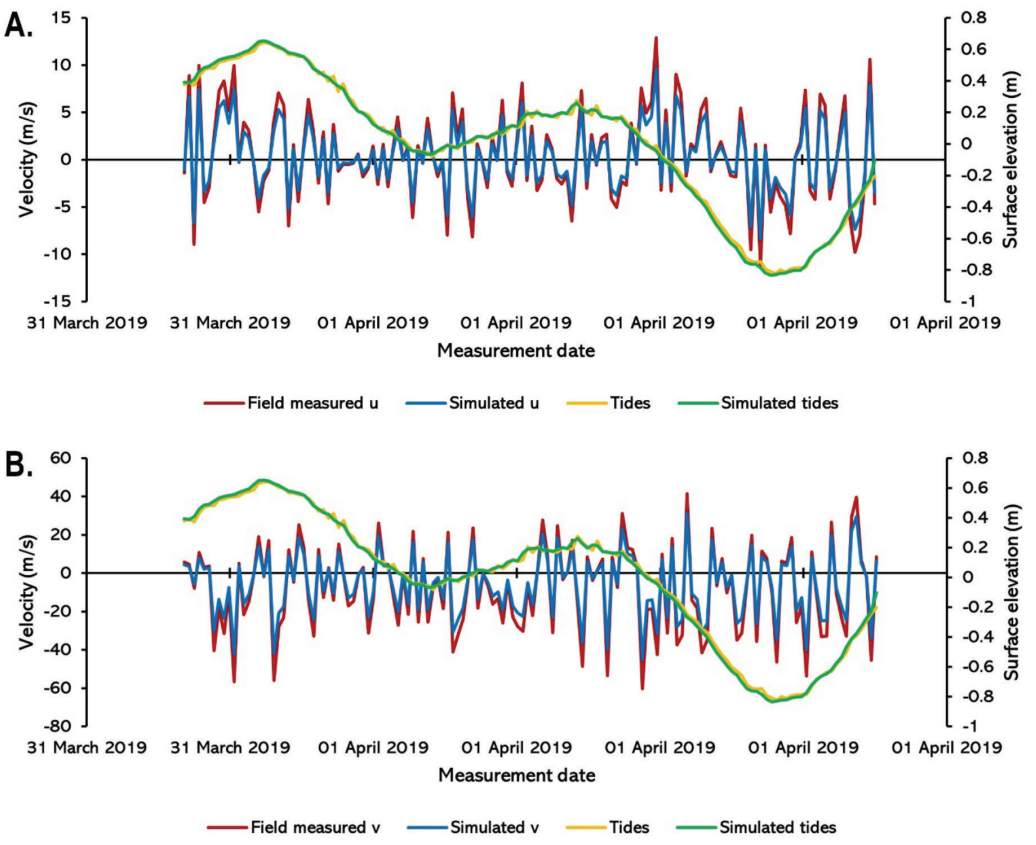

Figure 4: Hydrodynamic model validation using current velocity and surface elevation data in the Pengudang Station (M1). Zonal velocity (A); Meridional velocity (B)

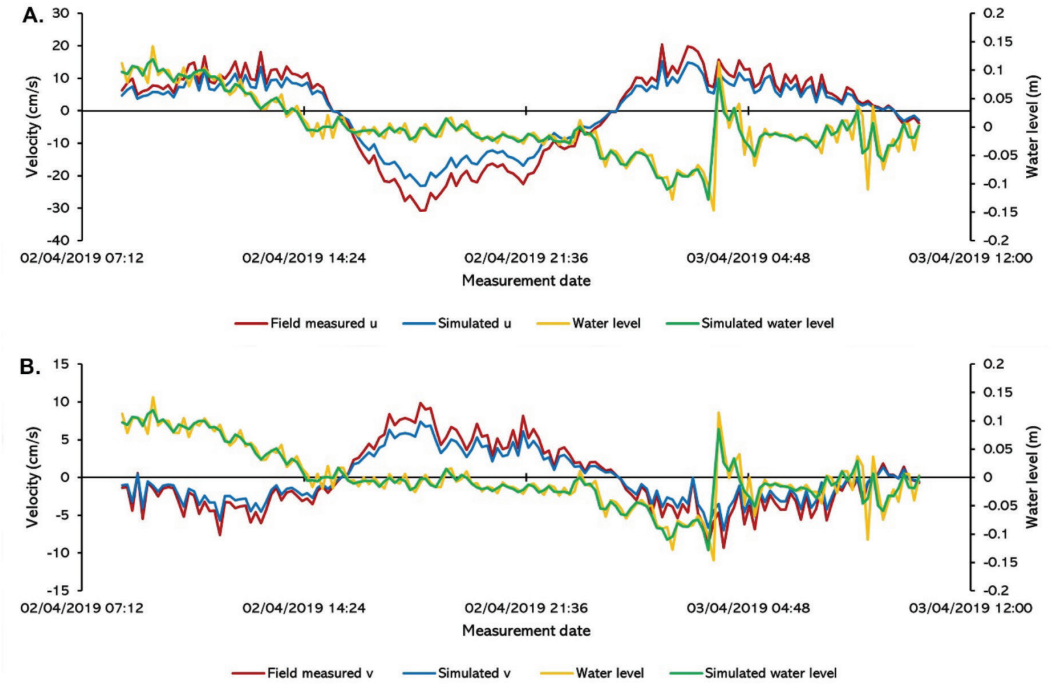

Figure 5: Hydrodynamic model validation using current velocity and surface elevation data in the Teluk Bakau Station (M2). Zonal velocity (A); Meridional velocity (B)

In the eastern station (Teluk Bakau), the current velocity component profile reflected a contrary pattern, and the water level data did not represent the tidal elevation since the instrument was deployed in the supper shallow area (Figure 5). Model and field measurement data have slightly different phases in terms of velocity fluctuation, ranging from 0.01 to 0.02 m/s. The RMSE obtained was more prominent than the northern station with 9.96% and 9.35% for the zonal and meridional components of current, respectively. Furthermore, changes in velocity between the zonal and meridional components of current tend to be more erratic, where during the positive phase of the zonal component, the negative value of the meridional component is observed and vice versa. This state indicates that the longshore and cross-shore transport can coincide, evoking higher vertical transport of suspended materials (Ye *et al.*, 2016).

The area of Teluk Bakau is strategic, where the influence of atmosphere-ocean interactions from the South China Sea on triggering local transport mechanisms is possible. However, the current component velocity profiles are more likely to reflect the impact of dynamic oceanographic factors in the coastal area. It is proven by the sufficiently high-velocity range of the zonal and meridional components, reaching 0.8 m/s and 0.2 m/s, respectively.

The remnant station is in the Madong area (southwestern part of Bintan Island). Unlike the current component's profile in Teluk Bakau, the fluctuation of current velocity in this station has a similar pattern even though the magnitudes were different, reflecting the tidal fluctuation (Figure 6). During flood tides, a sufficiently high current velocity moved toward the west and north, while during ebb tides, the opposite current flow took place.

The RMSE value gained from this comparison was 10.79% and 10.47% for the zonal and meridional components of current, respectively, with a deviation of approximately 0.1-0.3 m/s. The error value from this comparison shows that the model developed has some errors

either in the model input or the boundaries used in the model. The velocity of model data was significantly higher than the field-measured data. The zonal component of currents seems more arbitrarily erratic than the meridional one. This condition indicates that the horizontal transport toward the sea is predominant, triggering local sediment distribution, which may have less-sediment transport because the sediment movement is equal between its intake and resuspension (Li *et al.*, 2018).

Madong waters are categorised into semi-enclosed water areas where the oceanographic feature is supposed to be weak, but according to the measurement result, this water area has a relatively strong current flow specifically during the flood tide. Madong water area is surrounded by some small islands, possibly inducing a narrowed current circulation (bottleneck system), resulting in a higher velocity of water mass movement.

Hydrodynamic Model-based Estimation of TSS in Bintan Island

Simulation results between TSS and tidal current were overlaid into one map in Figure 7. During high tides [Figure 7 (A)], the easterly and southerly strong currents flowed landward, undergoing deformations due to many islands surrounding Bintan Regency. The current speed ranged from 0-0.5 m/s and moved toward the coastline throughout Bintan Island. The sea surface elevation is higher than the river surface elevation during flood tides, resulting in a low concentration of river-sourced suspended materials. Total Suspended Sediment (TSS) ranged from 1.4 to 15.2 mg/L.

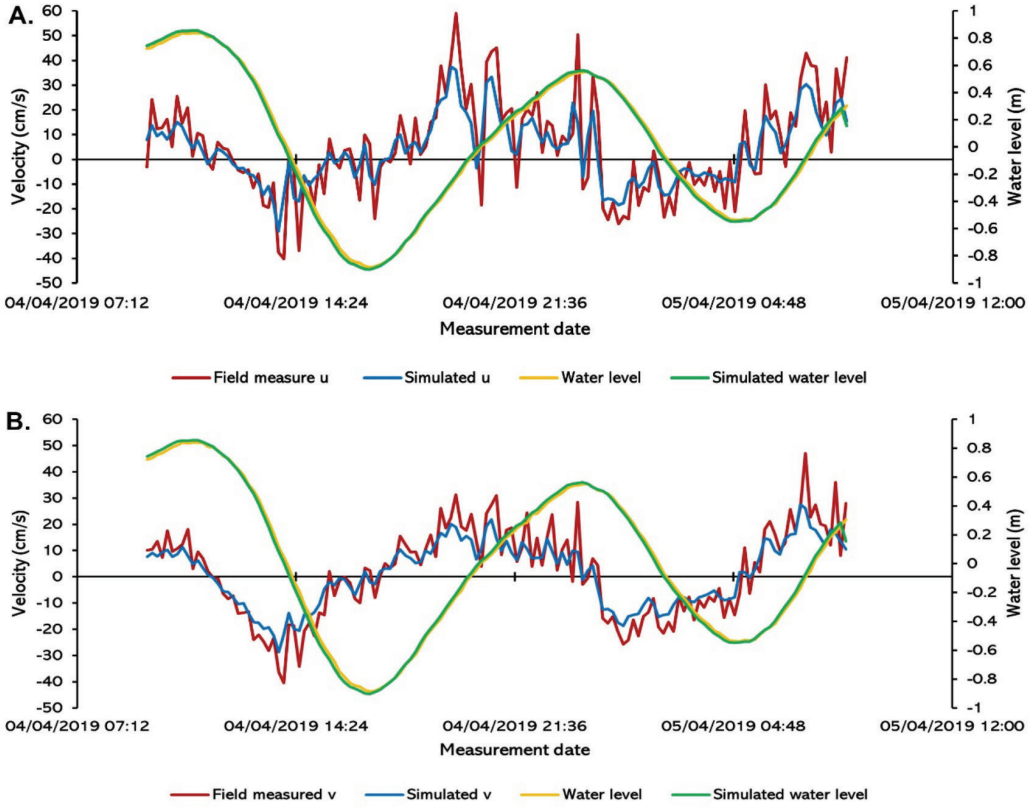

Figure 6: Hydrodynamic model validation using current velocity and surface elevation data in the Madong Station (M3). Zonal velocity (A); Meridional velocity (B)

Generally, a relatively high concentration of TSS was identified in the estuarine areas. In southwestern Bintan Island (in the surrounding Madong coastal area), the higher distribution of TSS occurs because of the existence of estuaries. A relatively high concentration of TSS was also observed in the northern part of Bintan Island. A more robust current feature in a narrowed area is predicted to affect the distribution of TSS in the semi-enclosed water area, while in the eastern part of Bintan Island (Teluk Bakau), the concentration of TSS tended to be lower because there are no rivers surrounding this area. In addition to Teluk Bakau, it is directly bordered by the South China Sea. This condition creates a consideration of sand sediment predomination. Therefore, the suspended sediment is minimal because of the coarse sediment transport predominance within a robust current environment (Zulfikar *et al.,* 2021).

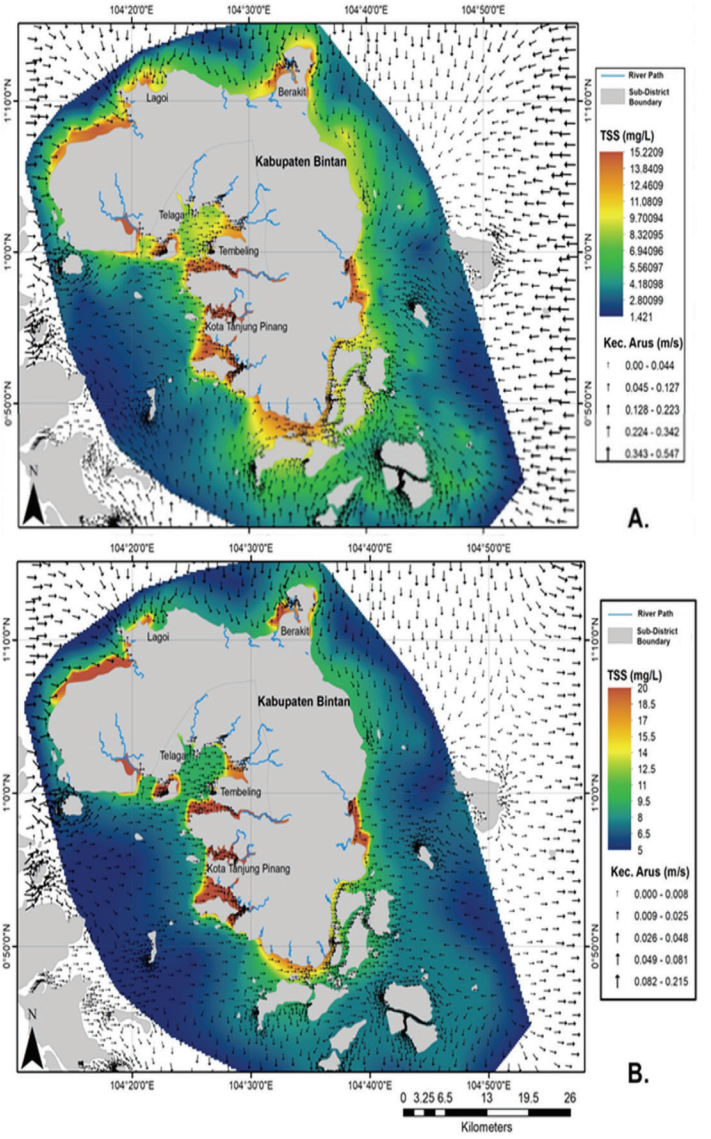

Figure 7: Hydrodynamic modelling result overlaid with simulated TSS concentration during flood tides (A) and ebb tides (B)

The same pattern of TSS distribution is also found during the low tidal condition. Generally, the existence of rivers and estuaries has an essential role in controlling suspended sediment throughout Bintan Coastline. However, the concentration of TSS was higher than during flood tides ranging from 5-20 mg/L. The weak current profile induces low transport of suspended materials. The current speed ranged from 0 to 0.21 m/s with a predominantly eastward erratic direction [Figure 7(B)]. On the other hand, this TSS simulation also shows that a higher concentration of TSS was observed in the southeastern and northern parts of Bintan Island. Concerning depositional processes of sediment, suspended sediment is quite arduous to settle just because of its fine-scaled size resulting in a more cohesive sediment predomination (Spencer *et al.*, 2019) and vice versa for coarse sediment (sand transport), whereby it will be quickly deposited in the bottom due to its larger mass (Layek *et al.,* 2018).

Sediment Transport Estimation

Unlike the TSS model, the sediment transport model simulates the distribution of coarse sediment in the three main study areas on Bintan Island. We applied two scenarios to predict total sediment transport along the coast in this simulation. The first scenario is the initial condition (red bar), while the second one is applying an obstacle likened to a seagrass ecosystem, which may potentially trap the coarse sediment effectively (blue bar) (Figure 8). The scenario was performed by applying a different value of the sediment drag coefficient (Saputra, 2014), as previously elucidated in the methodology.

Overall, Teluk Bakau station has an overwhelming sediment transport compared to the other stations, with 74.96 m^3/year. This state indicates that in the eastern part of Bintan Island (Teluk Bakau), the influence of the more dynamic physical factors from the South China Sea is possible. As mentioned in the previous subsection, the lowest concentration of TSS is observed in the Teluk Bakau area because this area is predominated by sand sediment. Concerning scenario 2, sediment transport decreases by around 19% per year, indicating that the existence of seagrass meadows can reduce the transportation of sediment and induce sedimentation. In Bintan Island's northern and southwestern parts (Pengudang and Madong), the annual sediment transport reached 39.83 and 7.24 m^3/year, respectively. These stations are interesting because while applying a variation of drag the coefficient of sediment in the model developed, transport sediment declines dramatically, reaching 19.03 m^3/year (52%) and 4.79 m^3/year (66 %), respectively. This condition is related to the current profile of Pengudang and

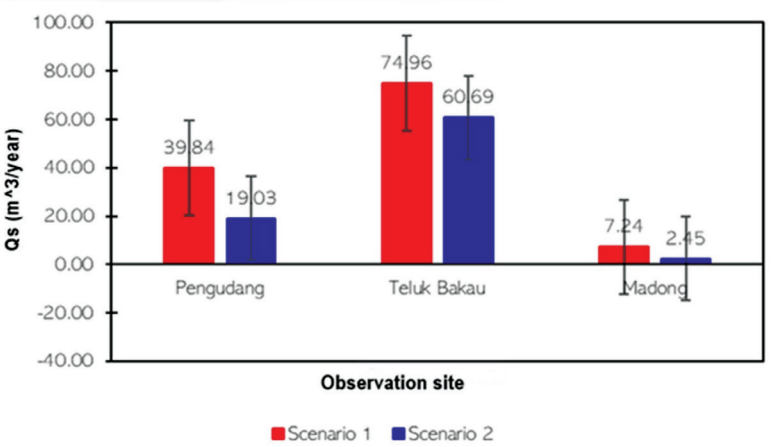

Figure 8: Sediment transport estimation based on hydrodynamic modelling. Scenario 1 (with seagrass) (blue) and Scenario 2 (without seagrass) (red)

Madong waters (see Figure 4 and Figure 6). The weak current profile induces a low transport so that both suspended and bed load sediment will ease to be deposited (Whinney *et al*., 2017). This condition is worsened by fewer scour and turbulence events so that the sedimentation process will be optimal in this area. In addition to the simulation result, the existence of seagrass meadows in those two areas can also significantly trap the sediment.

Figure 9 shows the monthly comparison between scenarios 1 and 2. Overall, percentage-wise, sediment transport changes are consistent with the annual transport (declined by about 20% due to the presence of seagrass meadow).

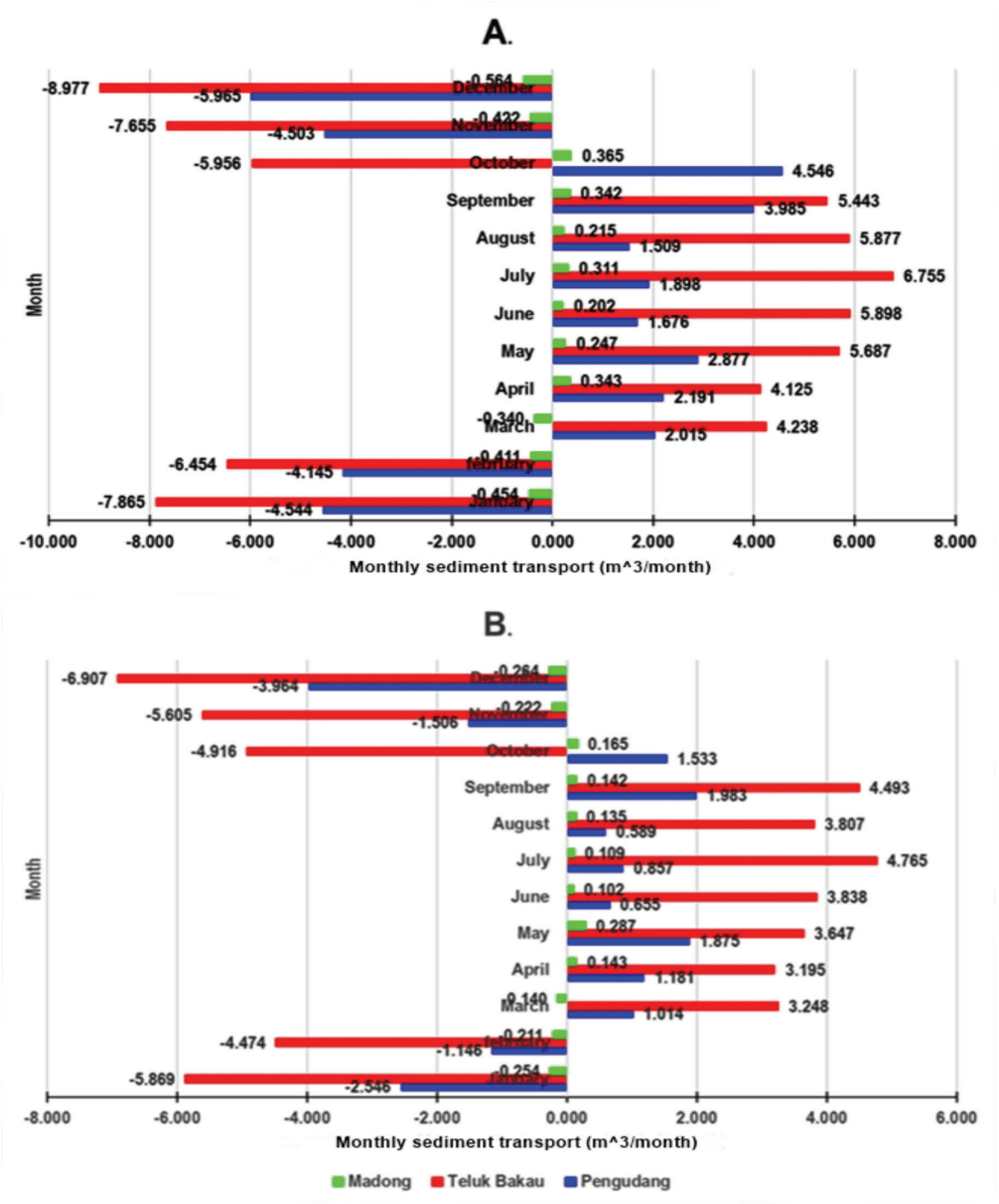

Figure 9: Monthly sediment transport estimation based on hydrodynamic modelling. Scenario 1 (without seagrass) (A) and Scenario 2 (with seagrass) (B)

The highest sediment transport was predicted to occur during southwest monsoons and vice versa for northeast monsoons. While, during the second transitional season, the sediment transport was higher than in the first transitional season. The dominant direction of local transport is also depicted in Figure 9 (A) and (B), by which, from March to September, sediment will predominantly move toward the right side from its sources. While, from October to February, sediment movement mostly moved toward the left side from its provenances. It indicates that the dominant wind movement and longshore transport have a significant role in triggering sediment transport (Whipple *et al*., 2018).

The anomaly was detected in March and October, where the transport direction was different from other months observed. The anomaly occurred at Madong station in March with an opposite transport dominant direction. In October, unlike the other observation stations, Teluk Bakau station experienced different transport directions where the leftward transport was predominant. The existence of seagrass meadows will trap the sediment and reduce the occurrence of scouring events. It can be seen in Figure 9 (B) that the sediment transport reduced significantly by about 25% in the Madong and Pengudang areas. While in the Teluk Bakau, the sediment transport slightly decreases (less than 5%).

We also simulated a prediction using scenario two, by which seagrass meadows will have existed for several future years. Of particular concern, sediment transport will gradually decrease by about 15% per year throughout 2019-2023 in Pengudang, Teluk Bakau, and Madong (Figure 10). This prediction is applied without any further changes in water conditions in Bintan Island so that different results are possible to occur according to many factors influencing the movement of sediment. Overall, based on the simulation developed, it concludes that seagrass or other natural creatures can significantly trap the sediment. Therefore, this result suggests that seagrass revitalisation can potentially recover an eroded area and make the coastal area more stable from the coastline change issue.

Conclusion

A higher concentration of Total Suspended Solids was generally observed seaward. The highest TSS distribution occurred in southwestern Bintan Island (in the surrounding Madong coastal area). A more robust current feature in a narrowed area may affect the high distribution of TSS in this semi-enclosed water area. The existence of rivers and estuaries also has an essential role in controlling the suspended sediment distribution. In contrast, the lowest concentration of TSS was observed in

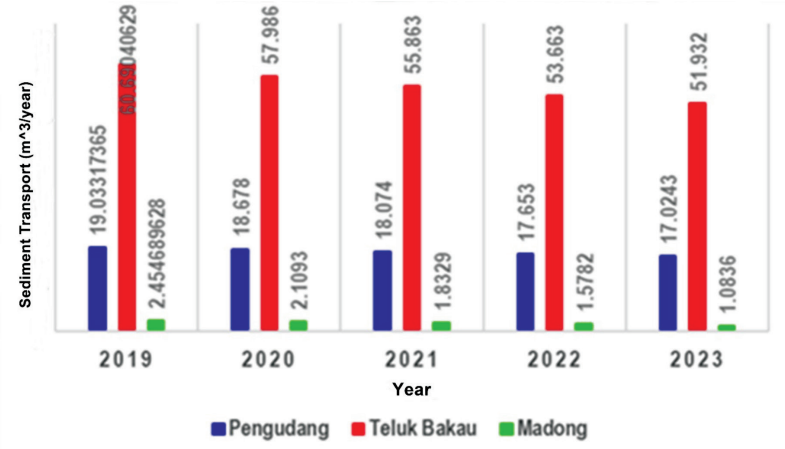

Figure 10: Sediment transport prediction applying scenario 2 considering the obstacle due to seagrass in the study area

the eastern part of Bintan Island (Teluk Bakau) due to the inexistence of rivers. The tidal current regimes control the distribution of suspended sediment and sediment transport along the coast.

Furthermore, Bintan Island is directly bordered by the South China Sea, where coarse sediment transport is predominant. Model simulation shows that the existence of seagrass meadows can significantly reduce the transportation of sediment and induce sedimentation. Therefore, this result triggers a consideration that seagrass meadow revitalisation could potentially be applied to an eroded area to recover faster and make the coastal area more stable from coastline changes.

Acknowledgements

We thank the Coral Reef Management and Rehabilitation Program-Coral Triangle Initiative (COREMAP-CTI) 2019 for funding this study.

References

Balqis, A. R. S., Yusoff, F. M., Arshad, A., & Nishikawa, J. (2016). Seasonal variations of zooplankton biomass and size-fractionated abundance about environmental changes in a tropical mangrove estuary in the Straits of Malacca. *Journal of Environmental Biology, 37*(4), 685695.

Bayhaqi, A., Fajari, A. K., Surinati, D., & Hidayati, N. (2021). Tidal current pattern in the surrounding Bintan Island Waters based on model simulation. In *International Conference on Sustainable Biomass (ICSB 2019)* (pp. 91-94). Atlantis Press.

Bong, C. W., & Lee, C.W. (2008). Nearshore and offshore comparison of marine water quality variables measured during SESMA 1. *Malaysian Journal of Science, 27*(3), 25-31.

Bozec, Y. -M., Acosta-Gonzales, G., Nunez-Lara, E., & Arias-Gonzalez, J. E. (2008). Impacts of coastal development on ecosystem structure and function of Yucatan coral reefs, Mexico. *Proceeding of the 11th International Coral Reef Symposium* Vol. 2 (Florida: Ft. Lauderdale 7-11 July 2008), 691-5.

Brodie, G., & N'Yeurt, A. D. (2018) Effects of climate change on seagrasses and seagrass habitats relevant to the Pacific Islands. *Science Review, 18*, 112-31.

Cea, L., Legout, C., Darboux, F., Esteves, M., & Nord, G. (2014). Experimental validation of a 2D overland flow model using high resolution water depth and velocity data. *Journal of Hydrology, 513*, 142-153. https://doi.org/10.1016/j.jhydrol.2014.03.052

De Boer, W. F. (2007). Seagrass-sediment interactions, positive feedbacks and critical thresholds for occurrence: A review. *Hydrobilogia*, *591*, 5-24.

Duarte, C. M. (2002). The future of seagrass meadows. *Environmental Conservation, 29*(2), 192-206. https://doi.org/10.1017/S0376892902000127

Fattah, A. H., Suntoyo, Dameriannne, H. A., & Wahyudi. (2018). Hydrodynamic and sediment transport modelling of Suralaya Coastal Area, Cilegon, Indonesia. *IOP. Conferences Series: Earth and Environmental Sciences, 135*, 012024.

Fischer, G., Karstensen, J., Romero, O.E., Baumann, K. D. B., Hefter, J., Mollenhauer, G., Iversen, M. H., Fiedler, B., Monteiro, I., & Körtzinger, A. (2016). Bathypelagic particle flux signatures from a suboxic eddy in the oligotrophic tropical North Atlantic: Production, sedimentation, and preservation. *Biogeosciences, 13*(11), 3203-3223.

Hamra, A. J. A., & Patria, M. P. (2019). Microplastic in Gonggong snails (*Laevistrombus turturella*) and sediment of Bintan Island, Kepulauan Riau Province, Indonesia. In *AIP Conference Proceedings*, *2202*(1), p. 020079. AIP Publishing LLC.

Harley, C. D. G., Hughes, A. R., Hultgren, K. M., Miner, B. G., Sorte, C. J. B., Thornber, C. S., Rodriguez, L. F., Tomanek, L., &

Williams, S. L. (2006). The impact of climate changes in coastal marine systems. *Ecology Letters, 9*(2), 228-41.

Irawan, S. (2017). Kondisi hidro-oseanografi perairan Pulau Bintan (studi kasus perairan Teluk Sasah). *Jurnal Kelautan: Indonesian Journal of Marine Science and Technology*, *10*(1), 41-53.

Karlina, I., Kurniawan, F., & Idris, F. (2018). Pressures and status of seagrass ecosystem in the coastal areas of North Bintan, Indonesia. *E3S Web of Conferences, 2nd Scientific Communication in Fisheries and Marine Sciences (SCiFiMaS 2018), 47*, 04008.

Kuriandewa, T. E., & Supriyadi, I. H. (2006). Seagrass mapping in East Bintan coastal area, Riau archipelago, Indonesia. *Coastal marine science*, *30*(1), 154-161.

Layek, M. K., Debnath, P., Sengupta, P., & Mukherjee, A. (2018). Delineation of sedimentary facies and groundwater-sea water disposition in an intertidal zone of the Bay of Bengal using GPR and VES. *Journal of Environmental and Engineering Geophysics, 23*(2), 235-49.

Li, J., Zheng, H., Xie, L., Zheng, Q., Ling, Z., & Li, M. (2021). Response of total suspended sediment and chlorophyll-a concentration to late autumn typhoon events in the Northwestern South China Sea. *Remote Sensing, 13*(15)*,* 2863. https://doi.org/10.3390/rs13152863

Li, Y., Jia, J., Zhu, Q., Cheng, P., Gao, S., & Wang, Y. P. (2018). Differentiating the effects of advection and resuspension on suspended sediment concentrations in a turbid estuary. *Marine Geology, 403*, 179-90.

Maeztu, I. Z., Matheson, F. E., Manley-Harris, M., Davies-Colley, R. J., Oliver, M., & Hawes, I. (2020). Effects of fine sediment on seagrass meadows: A case study of Zostera muelleri in Pauatahamui inlet, New Zealand. *Journal of Marine Science and Engineering*, *8*, 645.

Moeini, M. H., Etemad-Shabidi, A., & Chegini, V. (2010). Wave modelling and extreme value analysis off the Northern coast of the Persian Gulf. *Applied Ocean Research, 32*(2), 209-218.

Moriarty, D. J. W., & Boon, P. 1. (1989). Interactions of seagrass with sediment and water. In Larkum A. W. D., & Sheppard S. A. (Eds). *Biology of seagrasses* (pp. 500-535). Amsterdam: Elsevier.

Nursanti, Riniatsih, I., & Satriadi, A. (2013). Studi hubungan kerapatan vegetasi lamun dengan laju sedimentasi di Perairan Teluk Awur dan Bandengan Jepara pada periode Juni-Juli 2012. *Journal of Marine Research, 2*, 25-34.

Orth, R. J., Carruthers, T. J. B., Dennison, W. C., Duarte, C. M., Fourqurean, J. W., Heck, K. L., Hughes, A. R., Kendrick, G. A., Kenworthy, W., Olyarnik, S., Short, F. T., Waycott, M., & Williams, S. L. (2006). A global crisis for the seagrass ecosystem. *Bioscience, 56*(12), 987-996.

Saket, A., Etemad-Shahidi, A., & Moeini, M. H. (2013). Evaluation of ECMWF wind data for wave hindcast in Chabahar zone. *Journal of Coastal Research*, *65*(1), 380-385. https://doi.org/10.2112/SI65-065.1

Saputra, R. (2014). *Pengaruh Padang Lamun terhadap laju sedimen transpor dan perubahan garis pantai di Pantai Gumicik, Kabupaten Gianyar, Bali.* [Doctoral's Dissertation, Institut Teknologi Sepuluh Nopember].

Sarmada, I. F., Jaya, Y. V., Putra, R. D., & Suhana, M. P. (2018). Pemodelan pola arus di kawasan pesisir Pantai Kawal Kabupaten Bintan. *Dinamika Maritim*, *7*(1), 1-10.

Setyobudiandi, I., & Boer, M. (2021). Seagrass distribution in the East Coast of Bintan. *In IOP Conference Series: Earth and Environmental Science, 782*(4), p. 042001. IOP Publishing.

Signell, R. P., Carriel, S., Cavaleri, L., Chiggiato, J., Doyle, J. D., Pullen, J., & Sclavo, M.

(2005). Assessment of wind quality for oceanographic modelling in semi-enclosed basins. *Journal of Marine Systems, 53*, 217-233.

Solihuddin, T., Prihantono, J., Mustikasari, E., & Husrin, S. (2020). Dynamics of shoreline changes in the coastal region of Banten Bay and surrounding areas. *Jurnal Geologi Kelautan, 18*(2), 77-86.

Spencer, K. L., Wheatland, J., Manning, A. J., Gu, C., Carr, S., Botto, L., & Bushby, A. J. (2019). *Novel 3D observational data for estuarine sediment flocs: New understanding of cohesive sediment structure and behaviour*. *AGUFM* EP11A-01. American Geophysical Union.

Suhana, M. P., Nurjaya, I. W., & Natih, N. M. N. (2018). Karakteristik sedimen Pantai Timur Pulau Bintan provinsi Kepulauan Riau. *Dinamika Maritim*, *7*(1), 50-53.

Supriyadi, I. H., Rositasari, R., & Iswari, M. Y. (2018). The impact of land uses changes toward the seagrass condition in the East sea waters of Bintan Island, Riau Archipelago. *Jurnal Segara, 14*(1), 1-10.

Suratman, S., Hussein, A. N. A. R., Latif, M. T., & Weston, K. (2014). Reassessment of physico-chemical water quality in Setiu Wetland, Malaysia. *Sains Malaysiana, 43*(8), 1127–1131.

Suryansyah, Y. (2013). Potensi energi arus laut untuk pembangkit tenaga listrik di pulau-pulau kecil (Studi: Pulau Mantang di Bintan, Pulau Abang di Batam, dan Pulau Sugi di Karimun, Propinsi Kepulauan Riau). *Jurnal Kelautan Nasional*, *8*(1), 27.

Wahyudin, Y., Tridoyo, K., Adrianto, L., & Wardiatno, Y. (2018). A social ecological system of recreational fishing in the seagrass meadow conservation area on the East Coast of Bintan Island, Indonesia. *Ecological Economics, 148*, 22-35.

Waycott, M., Longstaff, B. J., & Mellor, J. (2005). Seagrass population dynamics and water quality in the Great Barrier Reef region: A Review and future research directions. *Marine Pollution Bulletin, 51*, 343-350.

Wessel, P., & Smith, W. H. F. (1996). A global, self-consistent, hierarchical, high-resolution shoreline database. *Journal of Geophysical Research,* 101(B4), 8741-8743. https://doi.org/10.1029/96JB00104

Whinney, J., Jones, R., Duckworth, A., & Ridd, P. (2017). Continuous in situ monitoring of sediment deposition in shallow benthic environments. *Coral Reefs, 36*(2), 521-33.

Whipple, A.C., Luettich Jr, R.A., Reynolds-Fleming, J.V. & Neve, R.H. (2018). Spatial differences in wind-driven sediment resuspension in a shallow, coastal estuary. *Estuarine, Coastal and Shelf Science, 213*, 49-60.

Wisha, U. J., Al Tanto, T., Pranowo, W. S., & Husrin, S. (2018). The current movement in Benoa Bay water, Bali, Indonesia: Pattern of tidal current changes simulated for the condition before, during, and after reclamation. *Regional Studies in Marine Science*, *18*, 177-187.

Wisha, U.J., Al Tanto, T., Pranowo, W., Husrin, S. & Kusumah, G. (2019). Numerical simulation of ocean wave using high-order spectral modeling techniques: Its influence on transport sediment in Benoa Bay, Bali, Indonesia. *Omni-Akuatika 15*(2), 20-35.

Wisha, U. J., Wijaya, Y. J., & Hisaki, Y. (2022). Tidal bore generation and transport mechanism in the Rokan River Estuary, Indonesia: Hydro-oceanographic perspectives. *Regional Studies in Marine Science*, *52*, 102309.

Witasari, Y., Wibowo, S. P., & Helfinalis. (2020). Adaptasi masyarakat nelayan terhadap kerentanan fisik Pesisir Pulau Bintan. *Journal of Fisheries and Marine Research*, *4*(3), 428-435.

Xiang, K., Yang, Z., Huai, W., & Ding, R. (2019). Large eddy simulation of turbulent flow structure in a rectangular embayment

zone with different population densities of vegetation. *Environmental Science and Pollution Research*, *26*, 14583-14597.

Ye, F., Zhang, Y.J., Friedrichs, M.A., Wang, H.V., Irby, I.D., Shen, J. & Wang. Z. (2016). A 3D, cross-scale, baroclinic model with implicit vertical transport for the Upper Chesapeake Bay and its tributaries. *Ocean Modelling,* 107**,** 82-96.

Zulfikar, M., Nurdin, N., Aryanto, N. C. D., Syafri, I., Muljana, B., & Nur, A. A. (2021). Distribution of Subsurface Quaternary Sediment in South Bintan Island Waters as A Potential Heavy Mineral Placer or Rare Earth Element Deposit Based on Seismic Interpretation. *Bulletin of the Marine Geology*, 36(1), 381296.